

An Ion-impact Study of Singlet-Triplet Transitions in Ethylene and Alkyl-substituted Ethylenes

Yukinori SATO,* Kazuki SATAKE, and Hokotomo INOUE

Research Institute for Scientific Measurements, Tohoku University, Sanjo-machi, Sendai 980

(Received August 21, 1981)

The $T \leftarrow N$ ($\pi \rightarrow \pi^*$) transitions in ethylene, all of its methyl derivatives, and 1-butene were observed by means of He^+ -impact energy-loss spectroscopy. With a resolution of better than 0.1 eV, a vibrational structure was just resolved in the $T \leftarrow N$ excitation spectrum of ethylene. The $T \leftarrow N$ transition energy was measured for the alkyl-ethylenes with a lower resolution. The results are in good agreement with the electron-impact data, indicating that the vibro-rotational excitation due to the impulsive momentum transfer is negligible in the present method. The $T \leftarrow N$ excitation cross-sections were found to decrease by half upon the unit substitution of alkyls. The relative invariance of the $T \leftarrow N$ transition energy and the decrease in the $T \leftarrow N$ cross-sections upon alkyl substitution may be attributable to the decrease in the intra- and intermolecular Coulomb and exchange interactions between π - and π^* - orbitals.

The alkylation red shift has been of some interest in studies of the electronic spectra of ethylene and alkyl-substituted ethylenes.¹⁻³⁾ After earlier studies using optical spectroscopy,^{4,5)} electron-impact methods have been applied to observe the bathochromic shift in the spin-forbidden $T \leftarrow N$ ($\pi \rightarrow \pi^*$) transition for a series of fundamental mono-olefinic hydrocarbons.⁶⁻⁸⁾ It has been revealed that the shift is much smaller in the $T \leftarrow N$ transition than in the optically allowed $V, R \leftarrow N$ transitions.

Measurements of energy loss by ion impact have also proved to be useful for observing spin-exchange transitions.⁹⁻¹¹⁾ In the ion-impact method, a singlet-triplet transition of a target molecule is induced by electron exchange between the projectile ion and the target molecule. Therefore, the proton impact on a singlet spin-state molecule results in excitations only to singlet states, whereas the He^+ impact, for example, can induce both singlet-singlet and singlet-triplet transitions in the molecule. Under a suitable collision energy, the lowest energy singlet-triplet transition of a molecule may be observed as the most intense peak in the ion-impact spectrum. Moore and his co-workers have performed several ion-impact experiments in order to investigate the effect of substitution on the $T, V, R \leftarrow N$ transition energies in substituted ethylenes⁹⁾ and in methyl-substituted butadienes¹⁰⁾ and the effect of ring size on the $T, V, R \leftarrow N$ transition energies in cycloalkenes.¹¹⁾

In the present study, the He^+ -impact method was used for observing the $T \leftarrow N$ transition in ethylene and alkylethylenes. Semiempirical calculations of the transition energies were also performed in order to analyze the experimental results. The purposes of the present study were; (1) to achieve a better energy resolution in the ion-impact spectroscopy; (2) to accumulate systematic data by means of ion impact to see if the ion-impact and electron-impact methods are consistent in determining the $T \leftarrow N$ transition energy; (3) to obtain some insight into the cause of the alkylation red shift, and (4) to investigate the effect of alkylation on the cross-section of $T \leftarrow N$ excitation induced by the ion-molecule interaction.

Experimental

The apparatus consists of an ion source, a mass analyzer, an energy monochromator for the incident-ion beam, a collision cell, an energy analyzer for the scattered ions, and a detector. The projectile He^+ ions are produced in a low-voltage plasma source.¹²⁾ The ions extracted from the source are focused into a beam, mass-analyzed by means of a Wien filter (COLUTRON Model 300), and directed into the ion spectrometer which is schematically shown in Fig. 1.

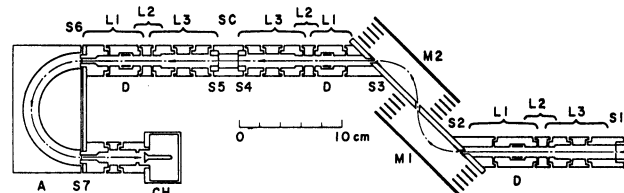


Fig. 1. Schematic of the ion spectrometer.

S1—S7: Apertures, L1: fixed ratio lens, L2: field lens, L3: variable ratio lens, D: beam steering deflectors, M1 and M2: parallel plate deflectors for an energy monochromator, SC: scattering cell, A: hemispherical energy analyzer, CH: channel electron multiplier.

The mass-analyzed beam is decelerated to an energy of 15–30 eV and focused into the electrostatic energy monochromator. The monochromator consists of two parallel-plate deflectors with an incident angle of $\pi/4$. The two deflectors are symmetrical in geometry and are directly connected so that they have a common inner plate. A coupling hole ($5 \times 10 \text{ mm}^2$) is bored at the center of the inner plate for the ion beam to pass from the first deflecting stage to the second deflecting stage. The entrance and the exit apertures (0.5 mm in diam.) are 116 mm apart and are held on the inner plate equidistantly from the coupling hole.

The ion beam transmitted through the monochromator is accelerated to an energy in the range of 2–3 keV through an acceleration-lens system and then enters into the collision cell. The target gas is introduced into the collision cell at a sufficiently low pressure to assure the single collision condition. The entrance and the exit apertures of the cell are 0.6 mm in diameter. The scattered ions are decelerated and focused onto the entrance aperture of the energy analyzer. The acceleration and deceleration of the ions are performed by means of a series of electrostatic cylinder lenses. The lenses

consist of a variable ratio lens (L1) and a fixed ratio lens (L3). An einzel lens (L2) is inserted as a field lens between the L1 and L3 lenses. The lenses are designed by using the optical properties of the two-element cylinder lens calculated by Read *et al.*¹³⁾

A hemispherical electrostatic deflector is used for the energy analyzer. The hemispheres are made of aluminum alloy. The mean radius of the outer and the inner hemispheres is 47.5 mm. The entrance and the exit apertures are 0.3 mm in diameter. The entrance aperture of the analyzer is 132 mm from the exit of the collision cell. The geometrical acceptance angle of the analyzer for scattered ions is 6.8×10^{-3} rad in a scattering plane, which is a measure of the present angular resolution. The voltage difference between the outer and inner hemispheres is held constant so as to pass ions at a constant transmission energy in the range of 15–30 eV.

After passing the analyzer, the ions are again accelerated and detected by a channel electron multiplier (MULLARD B318-AL).

The whole system is housed in connected metal vessels and pumped by means of oil-diffusion pumps. The ultimate pressure is 3×10^{-6} Pa, and the working background pressure is 5×10^{-4} Pa when the target gas and the ion-source gas are introduced.

An energy-loss spectrum is obtained by tracing the intensity of ions transmitted through the analyzer as a function of the deceleration potential between the collision cell and the analyzer. A voltage ramp applied to the deceleration lens is generated by a D/A converter, which is controlled by a personal-computer (SHARP MZ80-K). Output pulses from the detector are amplified, discriminated, and accumulated in the computer.

For a small-angle scattering at a high collision energy, the laboratory energy lost by the projectile is approximately given by:

$$\Delta E = (M_p/M_t)E\theta^2 + Q,$$

where M_p and M_t are the masses of the projectile and the target respectively; E is the laboratory collision energy; θ , the laboratory scattering angle, and Q , the change in the internal (vibrational, rotational, and electronic) energy. The term proportional to the collision energy, E , is the elastic loss due to the momentum transfer from the projectile to the target. The elastic loss can be minimized by observing the glancing collision at the forward scattering angle ($\theta=0$). The internal energy defect, Q , is also dependent on the scattering angle, because the vibro-rotational excitation, in addition to the vertical electronic excitation, is induced by the impulsive momentum transfer from the projectile to the target.^{14,15)} The degree of the impulsive vibro-rotational excitation is dependent on the impact parameter and can also be minimized in the forward scattering. In the present study, observations are made only for the forward scattering. Under the present angular resolution, the energy loss is expected to correspond to the vertical electronic transition energy, and the vibrational excitation is expected to follow the Franck-Condon principle. This is verified by the results to be presented in the following section. An overall energy resolution of better than 0.1 eV FWHM is achieved. This enables us to observe the vibrational structures in the electronic excitation spectrum of ethylene.

Results and Discussion

$T \leftarrow N$ Spectrum of Ethylene. The spectrum of ethylene in the energy-loss region from 3 to 6 eV is shown in Fig. 2. The spectrum was obtained with a

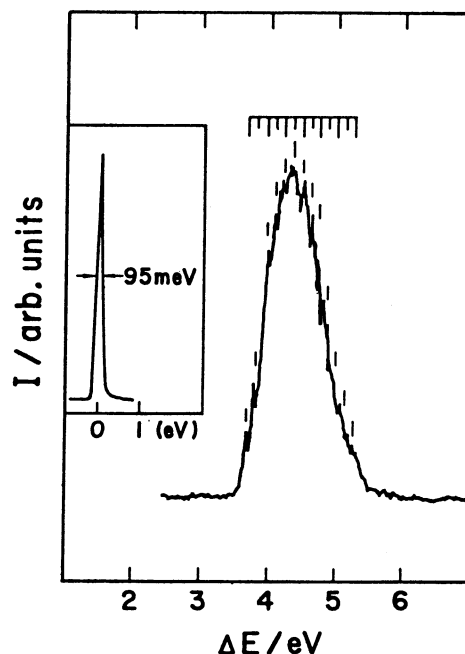


Fig. 2. Energy loss spectrum of ethylene by 2.3 keV He^+ impact. The inset shows the elastic peak.

resolution of 95 meV FWHM by the impact of 2.3 keV He^+ . A broad feature modulated by small structures appears with its maximum intensity at around 4.25 eV. The shape and position of the gross feature are in good agreement with those obtained by Moore.⁹⁾ The whole band has been assigned to the transition of ethylene from the ground state, N , to the lowest lying triplet state, T ($\pi \rightarrow \pi^*$). The small structures superimposed on the envelope are reproducible under the present resolution and show a spacing of 0.13 eV. The structures have an essential similarity, both in spacing and intensity distributions, with the high-resolution electron-impact spectrum obtained by Wilden and Comer,¹⁶⁾ though the present resolution is lower than theirs. The structures have been assigned to the vibrational progressions in the C–C stretching mode (ν_2). The spacing of 0.13 eV (1050 cm^{-1}) is the vibrational energy spacing of the ν_2 mode in the triplet state.

The similarity of the vibrational structures obtained from the ion-impact and electron-impact methods is evidence that the momentum transfer from the projectile to the target is not significant in the present observation; it can be thought, then, that the electronic excitation occurs in the Franck-Condon manner. The $T \leftarrow N$ excitation requires exchange interaction between the collision pair. It should be noticed that the exchange interaction, whose range is much shorter than the range of direct Coulomb interaction, is still effective in these glancing collisions.

Alkylation Shift in $T \leftarrow N$ Transition. The energy-loss spectra obtained by means of 2.5 keV He^+ impact are shown in Fig. 3 for ethylene, its six methyl derivatives, and an ethyl derivative. Because of a considerable decrease in the $T \leftarrow N$ excitation intensity in alkylethylenes, a lower resolution of about 0.35 eV FWHM was employed to accumulate these spectra. Common

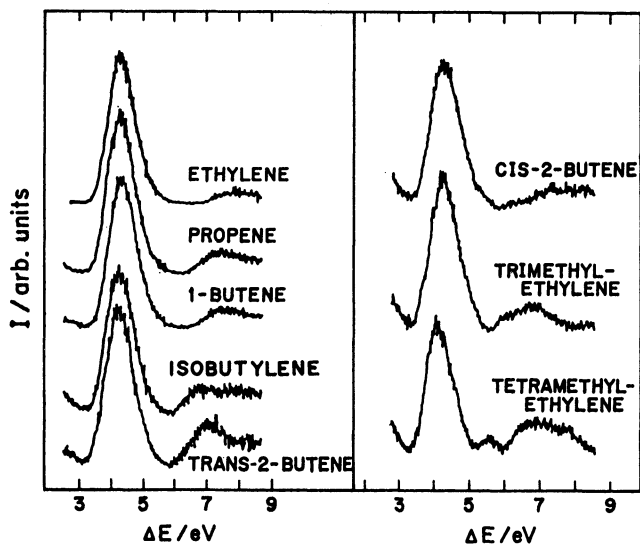


Fig. 3. Energy loss spectra of ethylene and alkyl-substituted ethylenes by 2.5 keV He^+ impact.

spectral features are seen for all of the alkylethylenes studied. The most intense $T \leftarrow N$ band at about 4.2 eV is followed by weaker $V, R \leftarrow N$ bands at higher-energy losses. The relative intensities of the $T \leftarrow N$ band and the $V, R \leftarrow N$ bands are dependent on the impact energy. The shape and position of the $T \leftarrow N$ band are relatively invariant with respect to the alkyl substitution, while the $V, R \leftarrow N$ bands rise at lower energies as the number

of substitution increases from zero to four. The separation of the $R \leftarrow N$ bands from the $V \leftarrow N$ band is not possible at this level of resolution, but the growth of the low-energy tail of the 7 eV peak with an increase in substitution may be attributable to the rapid red shift of the $2R \leftarrow N$ band.^{7,8)} A small peak at 5.5 eV is distinguishable in the tetramethylethylene; it has been assigned to the $2R \leftarrow N$ ($\pi \rightarrow 3s$) transition.^{7,8)} The position of the maximum intensity of the $T \leftarrow N$ band is listed in Table 1. Data obtained by the use of a variety of methods are included for comparison. The consistency of the present data with the electron-impact data indicates again that glancing collision without any significant momentum transfer is observed on these target molecules under the present scattering angular resolution. The present measurement gives an overall red shift of 0.20 eV for the $T \leftarrow N$ transition in going from ethylene to tetramethylethylene. The degree of shift in the $T \leftarrow N$ transition is much smaller than the corresponding 1.75 eV shift⁸⁾ in the $2R \leftarrow N$ transition.

Mulliken has indicated that the alkylation decrease in the ionization potential and the red shift in the $R \leftarrow N$ transition are largely attributable to a change in the effective nuclear charge of carbons due to charge transfer within the sigma system, while the red shift in the $V \leftarrow N$ transition may be entirely explained by the hyperconjugation in the pi system. The relative invariance of the $T \leftarrow N$ transition energy upon the alkylation has been predicted from VESCF-CI calculations by

TABLE 1. $T \leftarrow N$ TRANSITION ENERGY IN ALKYL-SUBSTITUTED ETHYLENES

Molecule	Vertical transition energy/eV					
	Present work ^{a)}	Other				
		Ion-impact ^{b)}	Electron-impact			Optical
Ethylene	4.25	4.3	4.32, ^{c)} 4.205, ^{g)}	4.30, ^{d)} 4.290, ^{g)}	4.2 ^{e)} 4.330 ^{g)}	4.6 ^{f)}
1-Butene	4.25	4.3				
Propene	4.25		4.28, ^{c)}	4.23, ^{d)}	4.35 ^{e)}	4.20 ^{b)}
Isobutene	4.20		4.22, ^{c)}	4.21 ^{d)}		4.09, ^{b)} 4.2 ^{d)}
cis-2-Butene	4.20	4.2	4.21, ^{c)}	4.21, ^{d)}	4.3 ^{e)}	4.2 ^{d)}
trans-2-Butene	4.20	4.2	4.24, ^{c)}	4.22, ^{d)}	4.4 ^{e)}	4.07, ^{b)} 4.2 ^{d)}
Trimethylethylene	4.15		4.16, ^{c)}	4.16 ^{d)}		3.70 ^{b)}
Tetramethylethylene	4.05		4.10, ^{c)}	4.05 ^{d)}		3.65 ^{b)}

a) The error of the peak position is estimated to be ± 0.05 eV. b) From Ref. 9. c) From Ref. 7. d) From Ref. 8. e) From Ref. 6. f) From Ref. 4. g) From Ref. 16. h) From Ref. 5. i) From Ref. 25.

TABLE 2. CALCULATED RESULTS FOR π - AND π^* -ORBITAL ENERGIES AND COULOMB AND EXCHANGE ENERGIES BETWEEN π - AND π^* -ORBITALS, AND $T \leftarrow N$ AND $V \leftarrow N$ TRANSITION ENERGIES
Units are in eV.

Molecule	$-\epsilon_\pi$	$\epsilon_\pi^* - \epsilon_\pi$	$J_{\pi\pi^*}$	$2K_{\pi\pi^*}$	$E(V \leftarrow N)^{a)}$	$E(T \leftarrow N)^{a)}$
Ethylene	11.158	11.377	7.740	4.934	7.581	3.637
Propene	10.429	10.647	7.054	4.188	7.324	3.385
Isobutylene	9.954	10.313	6.845	3.963	7.001	3.467
trans-2-Butene	10.066	10.064	6.613	3.741	6.797	3.235
cis-2-Butene	9.526	9.598	6.567	3.442	5.899	2.832
Tetramethylethylene	9.234	9.255	6.260	3.309	6.304	2.994

a) The transition energies are the CI results within single-excitation configurations.

Allinger *et al.*¹⁷⁾ and by Watson *et al.*¹⁸⁾ In order to see more specifically how this invariance arises, semiempirical calculations of the vertical $T \leftarrow N$ and $V \leftarrow N$ transition energies were performed by using a CNDO/S program made by Tajiri *et al.*¹⁹⁾ In the SCF level of the calculation, the $\pi \rightarrow \pi^*$ transition energy is given by;

$$E(T \leftarrow N) = (\epsilon_{\pi^*} - \epsilon_{\pi}) - J_{\pi\pi^*} \quad (1)$$

for the $T \leftarrow N$ transition and by;

$$E(V \leftarrow N) = (\epsilon_{\pi^*} - \epsilon_{\pi}) - J_{\pi\pi^*} + 2K_{\pi\pi^*} \quad (2)$$

for the $V \leftarrow N$ transition, where ϵ_{π} and ϵ_{π^*} are the SCF orbital energies and where $J_{\pi\pi^*}$ and $K_{\pi\pi^*}$ are, respectively, the Coulomb and the exchange energies between π - and π^* -orbitals. The calculated values for the quantities appearing in Eqs. (1) and (2) are listed in Table 2. The transition energies, $E(V \leftarrow N)$ and $E(T \leftarrow N)$, in the table are the results of partial configuration mixing within single-excitation configurations. The calculated results of $E(T \leftarrow N)$ are lower than the corresponding experimental data by more than 0.5 eV. This would be improved by taking the configuration mixing including double excitations at the expense of the worse agreement for the $V \leftarrow N$ transition energy.^{20,21)} Our attention will be confined to the gross results appearing in the SCF level. The differences $(\epsilon_{\pi^*} - \epsilon_{\pi})$ in the orbital energy, the Coulomb energy, and the exchange energy decrease altogether upon the methyl substitution. A remarkable point is that the degrees of change in $(\epsilon_{\pi^*} - \epsilon_{\pi})$, $J_{\pi\pi^*}$ and $2K_{\pi\pi^*}$ are all comparable in their magnitudes. Thus, the changes in $(\epsilon_{\pi^*} - \epsilon_{\pi})$ and $J_{\pi\pi^*}$ cancel each other to result in a small net change in the $T \leftarrow N$ transition energy upon the substitution. The changes in $J_{\pi\pi^*}$ and $K_{\pi\pi^*}$ may be taken to reflect, to some extent, the degree of hyperconjugation. The decrease in $(\epsilon_{\pi^*} - \epsilon_{\pi})$ arises mostly from the change in ϵ_{π} , which is largely attributable to the charge-transfer effect in the sigma system according to Mulliken. Thus, the relative invariance of the $T \leftarrow N$ transition energy arises from the cancellation of the hyperconjugation effect in $J_{\pi\pi^*}$ with the charge-transfer effect in $(\epsilon_{\pi^*} - \epsilon_{\pi})$, while the hyperconjugation effect in $K_{\pi\pi^*}$ remains, resulting in the red shift in the $V \leftarrow N$ transition to an extent similar to the decrease in $2K_{\pi\pi^*}$.

Alkylation Effect in $T \leftarrow N$ Excitation Cross-section.

It was found that the scattering intensity of the $T \leftarrow N$ excitation was considerably influenced by the alkyl substitution. The relative $T \leftarrow N$ cross-section decreases by almost half when the number of substitution increases by one. The $T \leftarrow N$ cross-section of 1-butene is nearly equal to that of propene. Three dimethylethylenes (*trans*- and *cis*-2-butene, and 2-methylpropene) have nearly identical $T \leftarrow N$ cross-sections. These facts indicate that the number of substitution is more important for the hypochromic effect than is either the size of a substituent or the site of substitution. It was also observed that the $V, R \leftarrow N$ cross-sections were less sensitive to the degree of substitution than were the $T \leftarrow N$ cross-sections. Quite the same hypochromic effect has been observed in the ion-impact study of methyl-substituted butadienes.¹⁰⁾

Mechanisms of excitation in heavy-particle collisions may be divided into two types.^{22,23)} In low-energy

collisions, an electronic excitation requires a close encounter of a collision pair. A quasi-molecular description and the potential crossing mechanism will be adequate for these collisions. In this mechanism, the threshold law of impact parameter holds and an excitation occurs for scattering angles larger than a threshold value. For high-energy collisions, on the other hand, excitations are possible in a distant encounter by means of the direct Coulomb or the exchange mechanism. Because of the delocalized character of the mechanism, one expects an excitation with no definite impact-parameter threshold. This is the case in the present experiment. The effective range of the ion-molecule interaction leading to the $T \leftarrow N$ excitation may be longer than the spatial extent of the surrounding alkyl groups. Otherwise, the momentum transfer between projectile and target would be considerable and would violate the vertical excitation. The spatial shielding effect does not seem to be important for the present hypochromic effect. We suggest that the hypochromic effect occurs through a change in the π - and π^* -wavefunctions upon the alkyl substitution, and that this in turn causes a decrease in the ion-molecule interaction. The exchange interaction for singlet-triplet transition²⁴⁾ includes an integral such as;

$$\langle \pi^*(1)\chi(2) | r_{12}^{-1} | \pi(2)\chi(1) \rangle, \quad (3)$$

where χ is the electronic wavefunction of the projectile He^+ ion and where r_{12} is the distance between the electrons to be exchanged. Since we have seen the decrease upon the substitution in the intramolecular Coulomb and exchange integrals between π - and π^* -orbitals, a decrease can also be expected in the ion-molecule exchange integral given by Eq. 3. The same reasoning leads to a decrease upon the substitution in the ion-molecule Coulomb interaction responsible for the $V, R \leftarrow N$ excitation. However, the alkylation decrease in the energy defect of the $V, R \leftarrow N$ excitation favors for an increase in the cross-section and makes the hypochromic effect less obvious than in the $T \leftarrow N$ excitation.

The authors wish to express their thanks to Dr. Noriyuki Shimakura for his help in the CNDO/S calculations. The present work was partially supported by a Grant-in-Aid for Scientific Research No. 454117 from the Ministry of Education, Science and Culture. The present work was also partially supported by the Nishina Memorial Foundation.

References

- 1) R. S. Mulliken, *Rev. Mod. Phys.*, **14**, 265 (1942).
- 2) A. J. Merer and R. S. Mulliken, *Chem. Rev.*, **69**, 639 (1969).
- 3) M. B. Robin, "Higher Excited State of Polyatomic Molecules," Academic Press, New York (1975), Vol. 2, Chap. IV, A, pp. 2-68.
- 4) D. F. Evance, *J. Chem. Soc.*, **1960**, 1735.
- 5) M. Itoh and R. S. Mulliken, *J. Phys. Chem.*, **73**, 4332 (1969).
- 6) D. F. Dance and I. C. Walker, *Proc. R. Soc. London, Ser. A*, **334**, 259 (1973).
- 7) W. M. Flicker, O. A. Mosher, and A. Kupperman,

Chem. Phys. Lett., **36**, 56 (1975).

- 8) K. E. Johnson, D. B. Johnston, and S. Lipsky, *J. Chem. Phys.*, **70**, 3844 (1979).
 - 9) J. H. Moore, Jr., *J. Phys. Chem.*, **76**, 1130 (1972).
 - 10) J. H. Moore, Y. Sato, and S. W. Staley, *J. Chem. Phys.*, **69**, 1092 (1978).
 - 11) I. Sauers, L. A. Grezzo, S. W. Staley, and J. H. Moore, *J. Am. Chem. Soc.*, **98**, 4218 (1976).
 - 12) M. Menzinger and L. Wahlin, *Rev. Sci. Instrum.*, **40**, 102 (1969).
 - 13) F. H. Read, A. Adams, and J. R. Soto-Monitiel, *J. Phys. E*, **4**, 625 (1971).
 - 14) H. Inouye, K. Niurao, and Y. Sato, *J. Chem. Phys.*, **64**, 1250 (1976).
 - 15) Y. Sato, K. Niurao, H. Takagi, and H. Inouye, *J. Chem. Phys.*, **65**, 3952 (1976).
 - 16) D. G. Wilden and J. Comer, *J. Phys. B*, **12**, L371 (1979).
 - 17) N. L. Allinger, J. C. Tai, and T. W. Stuart, *Theor. Chim. Acta*, **8**, 101 (1967).
 - 18) F. H. Watson, Jr., A. T. Armstrong, and S. P. McGlynn, *Theor. Chim. Acta*, **16**, 75 (1970).
 - 19) A. Tajiri, N. Ohmichi, and T. Nakajima, *Bull. Chem. Soc. Jpn.*, **44**, 2347 (1971).
 - 20) T. H. Dunning, W. J. Hunt, and W. A. Goddard, *Chem. Phys. Lett.*, **4**, 147 (1969).
 - 21) R. J. Buenker, S. D. Peyerimhoff, and W. E. Kammer, *J. Chem. Phys.*, **55**, 814 (1971).
 - 22) N. Andersen, T. Andersen, K. Bahr, C. L. Cocke, E. H. Pedersen, and J. O. Olsen, *J. Phys. B*, **12**, 2529 (1979).
 - 23) N. Andersen, "Electronic and Atomic Collisions," ed by N. Oda and K. Takayanagi, North-Holland, Amsterdam (1980), Proceedings of XIth ICPEAC, Kyoto, 1979, Invited Papers and Progress Reports, pp. 301—312.
 - 24) D. R. Bates and D. S. F. Crothers, *Proc. Phys. Soc.*, **90**, 73 (1967).
 - 25) F. H. Watson, Jr., and S. P. McGlynn, *Theor. Chim. Acta*, **21**, 309 (1979).
-